ICAS 2021 SHANG HAI
32nd Congress of the International Council of the Aeronautical Sciences
September 6-10, 2021 Pudong Shangri-La, Shanghai, China

Nonlinear Unsteady Aerodynamic Descriptions Based On Improved Goman's Model

Jing Yu[1], Xiao-jun Wu[1], Dong Hao[2*], Hong-yin Jia[1] & Shen-shen Liu[1]

[1]Computational Aerodynamics Institute, China Aerodynamics Research and Development Center, Mianyang, China
[2]Aerospace Technology Institute, China Aerodynamics Research and Development Center, Mianyang, China

Abstract

An advanced model of the nonlinear unsteady aerodynamic characteristics is presented based on Goman's state-space model in this paper. The progressive state-space description of Goman's model is improved and the nonlinearities of the attack angular rate and the flow separation position are considered and introduced. The nonlinear least square method (NLSM) is adopted to determine the unknown parameters in the developed model. The proposed modelling approach is verified by the wind tunnel data of NACA 0015 at four different attack angular rates, F18 aircraft at five different pitching rates, and F18 high alpha research vehicle (HARV) configuration at harmonic motions. The results indicate that the nonlinear unsteady aerodynamic properties of an aircraft could be expressed within the proposed modelling framework and the proposed nonlinear unsteady aerodynamic model could be directly applied to the flight simulation and control system designation of an aircraft.

Keywords: Nonlinear unsteady aerodynamic; State-space presentation; Angular rate of attack; Flow separation position; Nonlinear least square method

1. Introduction

It is one of the most significant problems to model the nonlinear unsteady aerodynamic forces and moments on an aircraft at high angles of attack [1, 2]. It is known to all that the nonlinear unsteady aerodynamic properties relate with the instant values of the variables and their historical values [3, 4]. Hence, the nonlinear unsteady aerodynamic model could be expanded by Taylor's series about some certain referential values [5, 6].

The accuracies of the nonlinear unsteady aerodynamic coefficients are required in development of aircraft [7-10]. A great deal of the literatures on that issue have been published before. Monfort et al. studied on F-4D's aerodynamic properties at static state in 1975 [11]. Utilizing a neural network modelling method, the aerodynamic coefficients of F-15 SMTD aircraft were determined by Peterson et al. [12]. Later, Greenwell published a survey of the aerodynamic modelling methods about the flight dynamics [13]. Combining GA (Genetic Algorithm) with the Euler method, additionally, Watanabe et al. carried out the optimization on the aerodynamic properties of a passenger plane [14]. Brunton et al., moreover, put forward a model with reduction of order to describe the lift coefficient of NACA 0006 at the Reynolds number of 65000 [15]. Then, Bagherzadeh et al developed a notional method based on the empirical mode decomposition algorithm (EMDA), to determine aerodynamic coefficients [16]. Notwithstanding, some investigations on the aerodynamic characteristics have been printed, such as Goman's model, none of them has considered the power items of the attack angular rate and the separation point position.

To model the nonlinearities of the unsteady aerodynamic coefficients, in this paper, a mathematical model is investigated based on improved Goman's model. The power items of the attack angular rate and the flow separation position are considered in the proposed model. The lift, drag, pitch moment coefficients and the parametric determination method are also analyzed. The given model describing the aerodynamic coefficients is validated by the wind tunnel measurements of three

* corresponding author: Dong Hao, haodongcardc@outlook.com

different physical models. The results disclose that the improved model has made a success of describing the aerodynamic characteristics. In a summary, the purpose of this paper are (i) to derivate an advanced aerodynamic modelling framework for the nonlinear unsteady properties and to identify the model parameters (Section 2), (ii) to validate the improved model from the measurements of three different physical models (Section 3), (iii) to give some conclusions in the end (Section 4).

2. Nonlinear unsteady aerodynamic descriptions and parameter determination

2.1 Improved Goman's model

For the dynamic angles of attack, the nonlinear unsteady aerodynamic characteristics show the hysteresis phenomenon. Such a hysteresis phenomenon can be usually described by a differential equation [17-21]. The modelling method of such hysteresis behaviors have been researched in our earlier literatures [22-30]. In this paper, an advanced state-space equation based on Goman's model is proposed to model such hysteresis characteristics. To describe the flow separation position, a state-space model expressed by a first-order differential equation was given by Goman [31-33]

$$\tau_1 \frac{dx}{dt} + x = f_0\left(\alpha - \tau_2 \dot{\alpha}\right) \tag{1}$$

The parameters in Eq. (1) and $f_0(\alpha)$ were given in [6, 30].

$$f_0(\alpha) = \frac{1}{1 + e^{\delta(\alpha - \alpha^*)}} \tag{2}$$

Adding the power items of $\dot{\alpha}$ and x into Eq. (1), an improved Goman's model is proposed as

$$\tau_1 \frac{dx}{dt} + x^{\gamma} = f_0\left(\alpha - \tau_2 \mathrm{sign}(\dot{\alpha})|\dot{\alpha}|^{v}\right) \tag{3}$$

where γ induces the nonlinearity of x. The plots of the static-state separation position for varying δ and the dynamic separation position for varying v have been given by Hao [30]. The simulated results of the dynamic separation position x for $\gamma = 1.0, 1.5, 2.0$ are plotted in Figure 1 ($v = 0.8$). As is displayed in Figure 1, it can be concluded that the parameter γ affects the curvilinear shape of x at larger angles of attack. x becomes larger as γ increases from 1.0 to 2.0. When $\gamma = 1.0$ and $v = 1.0$, the improved Goman's state-space equation becomes to the general Goman's model.

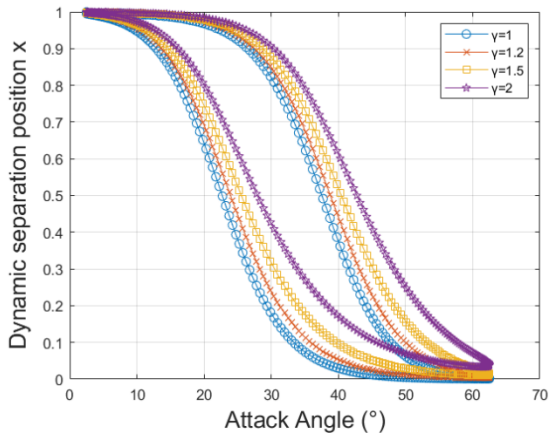

Figure 1 - Dynamic separation position for varying γ

2.2 Nonlinear unsteady aerodynamic descriptions

The nonlinear unsteady aerodynamic forces and moments relate with x, α, and $\dot{\alpha}$ [34-36]. Therefore, the nonlinear unsteady aerodynamic coefficients (lift, drag, pitch moment) are expressed as [30]

$$\begin{cases} C_L = C_L\left(x,\alpha,\dot{\alpha}\right) \\ C_D = C_D\left(x,\alpha,\dot{\alpha}\right) \\ C_m = C_m\left(x,\alpha,\dot{\alpha}\right) \end{cases} \tag{4}$$

The nonlinear unsteady aerodynamic coefficients are written as

$$\begin{aligned} C_L &= \underbrace{C_{L0} + C_{L\alpha}\left(x\right)\alpha + C_{L\alpha^2}\left(x\right)\alpha^2}_{C_{L,static}} + \underbrace{C_{Lq}\left(x\right)\dot{\alpha} + C_{Lq^2}\left(x\right)\dot{\alpha}^2 + C_{L\alpha q}\left(x\right)\alpha\dot{\alpha}}_{C_{L,dynamic}} \\ C_D &= \underbrace{C_{D0} + C_{D\alpha}\left(x\right)\alpha + C_{D\alpha^2}\left(x\right)\alpha^2}_{C_{D,static}} + \underbrace{C_{Dq}\left(x\right)\dot{\alpha} + C_{Dq^2}\left(x\right)\dot{\alpha}^2 + C_{D\alpha q}\left(x\right)\alpha\dot{\alpha}}_{C_{D,dynamic}} \\ C_m &= \underbrace{C_{m0} + C_{m\alpha}\left(x\right)\alpha + C_{m\alpha^2}\left(x\right)\alpha^2}_{C_{m,static}} + \underbrace{C_{mq}\left(x\right)\dot{\alpha} + C_{mq^2}\left(x\right)\dot{\alpha}^2 + C_{m\alpha q}\left(x\right)\alpha\dot{\alpha}}_{C_{m,dynamic}} \end{aligned} \tag{5}$$

where

$$\begin{cases} C_{L\alpha}\left(x\right) = a_1^L + b_1^L x + c_1^L x^2, C_{Lq}\left(x\right) = a_2^L + b_2^L x + c_2^L x^2, C_{L\alpha^2}\left(x\right) = a_3^L + b_3^L x + c_3^L x^2 \\ C_{Lq^2}\left(x\right) = a_4^L + b_4^L x + c_4^L x^2, C_{L\alpha q}\left(x\right) = a_5^L + b_5^L x + c_5^L x^2 \\ C_{D\alpha}\left(x\right) = a_1^D + b_1^D x + c_1^D x^2, C_{Dq}\left(x\right) = a_2^D + b_2^D x + c_2^D x^2, C_{D\alpha^2}\left(x\right) = a_3^D + b_3^D x + c_3^D x^2 \\ C_{Dq^2}\left(x\right) = a_4^D + b_4^D x + c_4^D x^2, C_{D\alpha q}\left(x\right) = a_5^D + b_5^D x + c_5^D x^2 \\ C_{m\alpha}\left(x\right) = a_1^m + b_1^m x + c_1^m x^2, C_{mq}\left(x\right) = a_2^m + b_2^m x + c_2^m x^2, C_{m\alpha^2}\left(x\right) = a_3^m + b_3^m x + c_3^m x^2 \\ C_{mq^2}\left(x\right) = a_4^m + b_4^m x + c_4^m x^2, C_{m\alpha q}\left(x\right) = a_5^m + b_5^m x + c_5^m x^2 \end{cases} \tag{6}$$

In Eq. (5), the aerodynamic coefficients are divided into two components: the static items and the dynamic items. In Eq. (6), additionally, $\left(a_i^j, b_i^j, c_i^j\right)$ with $i = 1,2,3,4,5$ and $j = L,D,m$ are the unknown parameters which could be identified by experiments or flight tests.

2.3 Parameter determination

For the static case, the static aerodynamic coefficients could be obtained by setting $\dot{\alpha} = 0$ in Eq. (5) as

$$\begin{aligned} C_{L,static} &= C_{L0} + C_{L\alpha}\left(x\right)\alpha + C_{L\alpha^2}\left(x\right)\alpha^2 \\ C_{D,static} &= C_{D0} + C_{D\alpha}\left(x\right)\alpha + C_{D\alpha^2}\left(x\right)\alpha^2 \\ C_{m,static} &= C_{m0} + C_{m\alpha}\left(x\right)\alpha + C_{m\alpha^2}\left(x\right)\alpha^2 \end{aligned} \tag{7}$$

$C_{L,static}^{Cal,i}$, $C_{D,static}^{Cal,i}$, and $C_{m,static}^{Cal,i}$ denote the calculated lift coefficient, drag coefficient and pitch moment coefficient at α_i, separately. $C_{L,static}^{Exp,i}$, $C_{D,static}^{Exp,i}$, and $C_{m,static}^{Exp,i}$ denote the measured lift coefficient, drag coefficient and pitch moment coefficient at α_i, respectively. Introducing MMSEC (Minimum Mean Square Error Combining), the static parameters are obtained by the optimization problem as

$$\min\ J = \left\| C_{static}^{Cal} - C_{static}^{Exp} \right\| = \sum_{i=1}^{N_L} \left| C_{L,static}^{Cal,i} - C_{L,static}^{Exp,i} \right|^2 + \sum_{i=1}^{N_D} \left| C_{D,static}^{Cal,i} - C_{D,static}^{Exp,i} \right|^2 + \sum_{i=1}^{N_m} \left| C_{m,static}^{Cal,i} - C_{m,static}^{Exp,i} \right|^2 \tag{8}$$

After gained the static parameters, the dynamic parameters can be calculated from the dynamic wind tunnel measurements. $C_{L,dynamic}^{Cal,i}$, $C_{D,dynamic}^{Cal,i}$, and $C_{m,dynamic}^{Cal,i}$ denote the calculated lift coefficient, drag coefficient and pitch moment coefficient at α_i, separately. $C_{L,dynamic}^{Exp,i}$, $C_{D,dynamic}^{Exp,i}$, and $C_{m,dynamic}^{Exp,i}$ denote the experimental lift coefficient, drag coefficient and pitch moment coefficient at α_i, respectively. Thus, the dynamic parameters are gained by

$$\min\ J = \left\| C_{dynamic}^{Cal} - C_{dynamic}^{Exp} \right\| = \sum_{i=1}^{N_L} \left| C_{L,dynamic}^{Cal,i} - C_{L,dynamic}^{Exp,i} \right|^2 + \sum_{i=1}^{N_D} \left| C_{D,dynamic}^{Cal,i} - C_{D,dynamic}^{Exp,i} \right|^2 + \sum_{i=1}^{N_m} \left| C_{m,dynamic}^{Cal,i} - C_{m,dynamic}^{Exp,i} \right|^2 \tag{9}$$

Solving the optimization problems of Eq. (8) and Eq. (9), NLSM (The Nonlinear Least Square Method) is utilized to solve the parameters. Overall, there are totally fifty-four parameters which should be gained from the wind tunnel measurements. Once the parameters are obtained, the nonlinear

unsteady aerodynamic forces and moments of an aircraft or airfoil can be predicted. The approach of the proposed modelling method is validated by three wind tunnel tests in the following section. The detailed parameter identification algorithm is displayed in Figure 2.

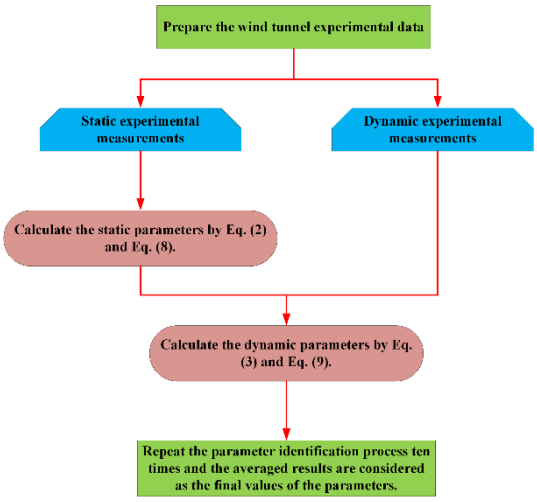

Figure 2 - Parameter identification algorithm

3. Verification

In this section, the measurements of NACA 0015 airfoil [34], F18 aircraft [35], and F18 HARV (High Alpha Research Vehicle) configuration [36] are adopted to validate the proposed aerodynamic model.

3.1 NACA 0015 airfoil

The aerodynamic experimental measurements of a NACA 0015 airfoil, supplied by Jumper et al. [34], are utilized to verify the proposed model. In Jumper et al.'s wind tunnel tests, the following formulas can be got.

$$\begin{aligned} &\alpha(t)=\dot{\alpha}(t)t, \quad 0\le\alpha(t)\le 38^{\circ} \\ &q(t)=\dot{\alpha}(t)=\text{constant} \end{aligned} \tag{10}$$

The static parameters and the dynamic parameters could be obtained by the Eq. (11) and (12).

$$\min\ J=\left\|C_{static}^{Cal}-C_{static}^{Exp}\right\|=\sum_{i=1}^{N_{Ls}}\left|C_{L,static}^{Cal,i}-C_{L,static}^{Exp,i}\right|^2 \tag{11}$$

$$\min\ J=\left\|C_{dynamic}^{Cal}-C_{dynamic}^{Exp}\right\|=\sum_{j=1}^{4}\sum_{i=1}^{N_{Lj}}\left|C_{L,dynamic}^{Cal,i}\left(\dot{\alpha}_j\right)-C_{L,dynamic}^{Exp,i}\left(\dot{\alpha}_j\right)\right|^2 \tag{12}$$

where N_{Ls} is the static points, N_{Lj} is the dynamical points at $\dot{\alpha}_j$. The determined parameters of the proposed model for the lift coefficient in Eq. (5) are illustrated in Table 1. The static and dynamic results are separately depicted in Figure 3 and Figure 4. The values of the illustrated parameters in Table 1 are solved according to Eq. (11) and Eq. (12) by NLSM.

Table 1 - Determined values of NACA 0015

Variable	Value
δ	0.4150
α^*	9.6958
τ_1	−0.6243
τ_2	5.5678
v	−0.1162
γ	0.8639
C_{L0}	−0.0090
$C_{L\alpha}(x)$	$0.1995+0.051545x-0.1826x^2$

$C_{Lq}(x)$	$-1.0410+0.5189x+0.5220x^2$
$C_{L\alpha^2}(x)$	$-0.008246-0.01846x+0.02085x^2$
$C_{Lq^2}(x)$	$0.07050-0.1400x+0.06952x^2$
$C_{L\alpha q}(x)$	$0.03390+0.03648x-0.07030x^2$

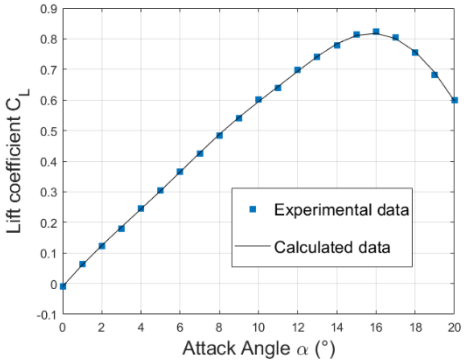

Figure 3 - The static results of NACA 0015 airfoil

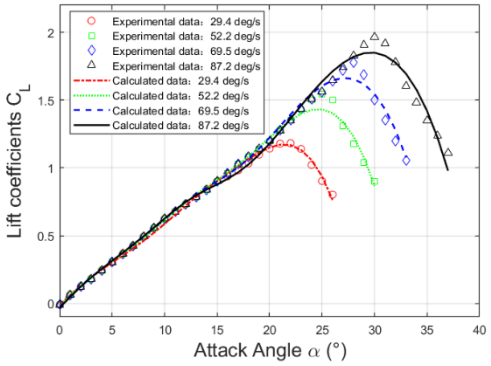

Figure 4 - The dynamic results of NACA 0015 airfoil

As is seen in Figure 3 and Figure 4, the measured aerodynamic data of NACA 0015 airfoil are from the reference and the simulated results are obtained by Eq. (3) and Eq. (5) with the parameters in Table 1. In Figure 3 and Figure 4, it can be seen that the proposed aerodynamic model excellently expresses the static and dynamic lift coefficients versus the angle of attack and the angular rate of attack. The simulated data of the lift coefficient have a well agreement with the experimental data of NACA 0015 airfoil at four different angular rate of attack, i.e. 29.4 degree/s, 52.2 degree/s, 69.5 degree/s, and 87.2 degree/s. The aerodynamic coefficients of NACA 0015 airfoil can be described by the proposed nonlinear unsteady aerodynamic model.

3.2 F18 aircraft

In addition, to verify the obtained aerodynamic model suitable for a full model of aircraft while not just an airfoil, the experimental data of Brandon are selected [35]. In Brandon's test, we have

$$\begin{aligned} &\alpha(t)=\dot{\alpha}(t)t, \quad 5^\circ \le \alpha(t) \le 75^\circ \\ &q(t)=\dot{\alpha}(t)=\text{constant} \end{aligned} \tag{13}$$

The static type of parameters in the proposed model are determined from the aerodynamic data of $\dot{\alpha}(t)=0$ by solving Eq. (11) and the dynamic type of parameters in the proposed model are identified from the wind tunnel data at five different angular rates of attack, i.e. $\dot{\alpha}_1(t)=57.8\,\text{deg/s}$, $\dot{\alpha}_2(t)=115.0\,\text{deg/s}$, $\dot{\alpha}_3(t)=172.8\,\text{deg/s}$, $\dot{\alpha}_4(t)=-57.8\,\text{deg/s}$, and $\dot{\alpha}_5(t)=-115.0\,\text{deg/s}$, by solving the following optimization problem.

$$\min\ J=\left\|C_{dynamic}^{Cal}-C_{dynamic}^{Exp}\right\|=\sum_{j=1}^{5}\sum_{i=1}^{N_{Lj}}\left|C_{L,dynamic}^{Cal,i}\left(\dot{\alpha}_j\right)-C_{L,dynamic}^{Exp,i}\left(\dot{\alpha}_j\right)\right|^2 \tag{14}$$

The obtained parameters from Brandon's data are listed in Table 2 and the results of the lift coefficient are plotted in Figure 5 and Figure 6, respectively. As is shown in Figure 5 and Figure 6, the advanced nonlinear unsteady aerodynamic model is able to describe both the static and dynamic aerodynamic coefficients of F18 aircraft. The calculated results of the present model have a nice agreement with the wind tunnel experiments, both for the static and dynamic conditions at different pitching rates of 57.8 degree/s, 115.0 degree/s, 172.8 degree/s, -57.8 degree/s, and -115.0 degree/s. More importantly, it can be also concluded that the surrounded area of the hysteresis curve becomes larger with the angular rate of attack increasing. That is to say the area surrounded by the hysteresis curve of $|\dot{\alpha}| = 115.0$ degree/s is larger than that of $|\dot{\alpha}| = 57.8$ degree/s.

Table 2 - Determined values of F18 aircraft

Variable	Value
δ	0.2446
α^*	47.2306
τ_1	−11.7493
τ_2	−91.2781
v	−0.4310
γ	7.1775
C_{L0}	0.03598
$C_{L\alpha}(x)$	$0.03781 - 0.1367x + 0.1694x^2$
$C_{Lq}(x)$	$0.3629 - 0.3766x + 0.01450x^2$
$C_{L\alpha^2}(x)$	$-4.0161\times10^{-4} + 0.003320x - 0.003502x^2$
$C_{Lq^2}(x)$	$-0.003508 + 0.009566x - 0.006059x^2$
$C_{L\alpha q}(x)$	$0.02214 - 0.04559x + 0.02353x^2$

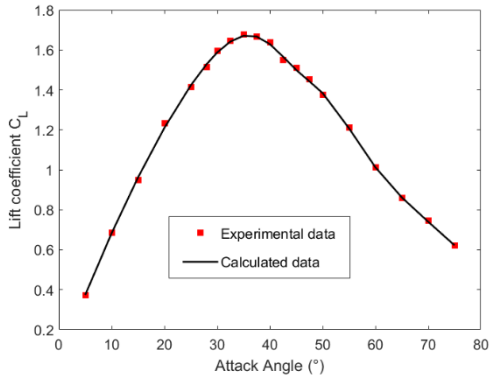

Figure 5 - The static results of F18 aircraft

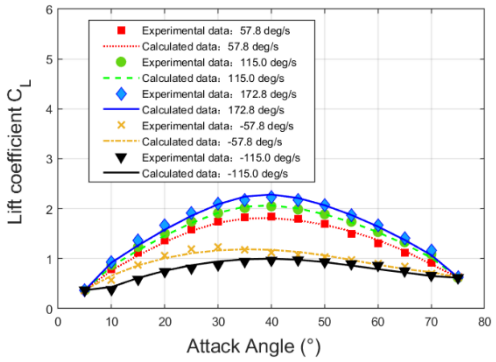

Figure 6 - The dynamic results of F18 aircraft

3.3 F18 HARV configuration

In the above, the developed aerodynamic model is validated by the wind tunnel experimental measurements at constant angular rate. Then, the present model is furtherly validated by the

aerodynamic data of F18 HARV configuration at harmonic motion from Hu et al. [36]. The law of the attack angle is

$$\begin{cases} \alpha(t) = 32.5 - 30\cos\omega t \\ \dot{\alpha}(t) = 30\omega\sin\omega t \end{cases} \tag{15}$$

The static parameters can be calculated by

$$\min \ J = \sum_{i=1}^{N_{Ls}} \left| C_{L,static}^{Cal,i} - C_{L,static}^{Exp,i} \right| + \sum_{i=1}^{N_{Ds}} \left| C_{D,static}^{Cal,i} - C_{D,static}^{Exp,i} \right| + \sum_{i=1}^{N_{ms}} \left| C_{m,static}^{Cal,i} - C_{m,static}^{Exp,i} \right| \tag{16}$$

where N_{Ls}, N_{Ds}, and N_{ms} are the number of static measured points for the lift coefficient, drag coefficient and pitch moment coefficient, respectively. And the dynamic parameters can be obtained by solving the following optimizing problem

$$\min J = \sum_{i=1}^{N_{Ld}} \left| C_{L,dynamic}^{Cal,i} - C_{L,dynamic}^{Exp,i} \right| + \sum_{i=1}^{N_{Dd}} \left| C_{D,dynamic}^{Cal,i} - C_{D,dynamic}^{Exp,i} \right| + \sum_{i=1}^{N_{md}} \left| C_{m,dynamic}^{Cal,i} - C_{m,dynamic}^{Exp,i} \right| \tag{17}$$

where N_{Ld}, N_{Dd}, and N_{md} are the number of dynamic measured points for the lift coefficient, drag coefficient and pitch moment coefficient, respectively. The gained parameters are listed in Table 3 and the simulated static and dynamic results of the aerodynamic coefficients are displayed in Figure 7 and Figure 8, respectively.

Table 3 - Determined values of F18 HARV

Variable	Value
δ	0.1012
α^*	17.0077
τ_1	0.3041
τ_2	0.004251
v	1.1518
γ	1.0024
C_{L0}	0.095
$C_{L\alpha}(x)$	$0.003515 - 0.5960x + 0.7822x^2$
$C_{Lq}(x)$	$0.009542 - 0.01646x + 0.006050x^2$
$C_{L\alpha^2}(x)$	$2.8278\times10^{-5} + 0.02450x - 0.01033x^2$
$C_{Lq^2}(x)$	$9.3896\times10^{-7} - 9.9501\times10^{-8}x - 3.4711\times10^{-7}x^2$
$C_{L\alpha q}(x)$	$-1.5477\times10^{-4} - 6.9452\times10^{-4}x + 9.3021\times10^{-4}x^2$
C_{D0}	–0.048
$C_{D\alpha}(x)$	$0.02835 - 0.3614x + 0.4199x^2$
$C_{Dq}(x)$	$0.01161 + 0.02437x - 0.04475x^2$
$C_{D\alpha^2}(x)$	$-1.7671\times10^{-5} + 0.01115x - 0.006402x^2$
$C_{Dq^2}(x)$	$3.1282\times10^{-6} + 2.6991\times10^{-5}x - 1.3713\times10^{-5}x^2$
$C_{D\alpha q}(x)$	$-1.6666\times10^{-4} - 0.001738x + 9.8871\times10^{-4}x^2$
C_{m0}	–0.082
$C_{m\alpha}(x)$	$0.03471 - 0.06187x + 0.06181x^2$
$C_{mq}(x)$	$0.006746 + 0.007739x - 0.01901x^2$
$C_{m\alpha^2}(x)$	$-6.2481\times10^{-4} - 3.8901\times10^{-4}x + 2.9497\times10^{-4}x^2$
$C_{mq^2}(x)$	$5.6252\times10^{-8} + 1.5403\times10^{-5}x - 1.4043\times10^{-5}x^2$
$C_{m\alpha q}(x)$	$-1.1353\times10^{-4} - 6.7736\times10^{-4}x + 5.3338\times10^{4}x^2$

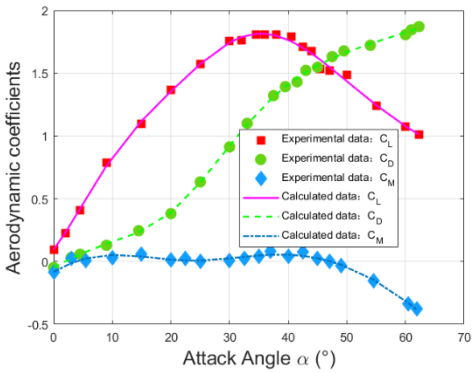

Figure 7 - The static results of F18 HARV

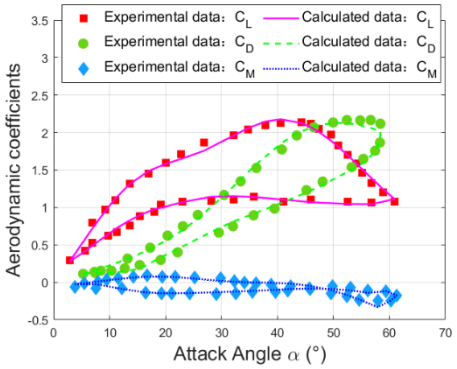

Figure 8 - The dynamic results of F18 HARV

As is described in Figure 7 and Figure 8, the proposed aerodynamic expression can model the aerodynamic forces and moments of an aircraft which pitches at a large-amplitude harmonic oscillation. The peak feature of the static lift coefficient and the hysteresis properties at dynamic angle of attack can be got in Figure 7 and Figure 8, separately. The calculated results of the proposed aerodynamic model with the identified parameters agree well with testing data.

In a summary, the proposed aerodynamic model has been validated by the wind tunnel data of Jumper, Brandon, and Hu with success. At a constant pitching rate and a harmonic pitching motion, the present model could represent the nonlinear unsteady aerodynamic behaviors of an aircraft. The novel aerodynamic model can be applied in a wide range and can be involved into the simulating and designing of aircraft. Such investigation of the present model owns a significant application prospect.

3.4 Models comparison

In this section, the developed model and the general Goman's model are compared and discussed based on the aerodynamic data of F18 HARV configuration used in section 3.3. The comparison results are depicted in Figure 9 and Figure 10. It can be seen from Figure 9 and Figure 10 that in some areas (e.g. the lower part of the curve in Figure 9), the present model can slightly better fitting the experimental data and the current model could be further improved.

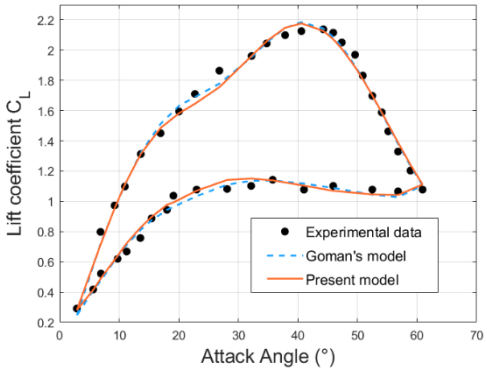

Figure 9 - Comparisons of lift coefficient between the Goman's model and the present model.

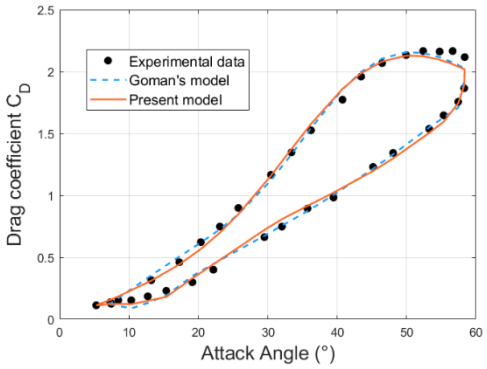

Figure 10 - Comparisons of drag coefficient between the Goman's model and the present model.

4. Conclusions

Based on improved Goman's model described by a first-order differential equation in [30], an advanced nonlinear unsteady aerodynamic model is put forward in the present paper. The aerodynamic model is represented and validated by the aerodynamic data of NACA0015 airfoil at four constant angular rates (Jumper's test), F18 aircraft at five constant pitching rates (Brandon's test), and F18 HARV at large-amplitude harmonic motion (Hu's test). The parametric identification method is also given in this paper. The results indicate that the simulated aerodynamic coefficients have a well agreement with the wind tunnel measurements for all selected cases. The proposed aerodynamic coefficients own a wide range of applicability and can be involved into the simulating and designing of aircraft. The novel aerodynamic modelling approach has a good engineering prospect.

5. Copyright Statement

References

[1] J. Tianfeng, G. Zhenghong, Unsteady aerodynamic modeling at high angles of attack, AIAA Atmospheric Flight Mechanics Conference, 2000. (DOI: AIAA-2000-3908)

[2] Y. Lyu, W. Zhang, J. Shi, et al, Unsteady aerodynamic modeling of biaxial coupled oscillation based on improved elm, Aerosp. Sci. Technol. 60 (2017) 58-67. (DOI: 10.1016/j.ast.2016.10.029)

[3] D.J. Linse, R.F. Stengel, Identification of aerodynamic coefficients using computational neural networks, 30th Aerospace Sciences Meeting & Exhibit, 1992. (DOI: AIAA 92-0172)

[4] J. Kou, W. Zhang, Multi-kernel neural networks for nonlinear unsteady aerodynamic reduced-order

modeling, Aerosp. Sci. Technol. 67 (2017) 309-326. (DOI: 10.1016/j.ast.2017.04.017)

[5] G.T. Chapman, L.A. Yates, Nonlinear aerodynamic parameter estimation and model structure identification, AIAA Atmospheric Flight Mechanics Conference, 1992. (DOI: AIAA 92-4502)

[6] Y. Fan, F.H. Lutze, Identification of an unsteady aerodynamic model at high angles of attack, 1996. (DOI: AIAA-96-3407-CP)

[7] G. Lin, C.E. Lan, J.M. Brandon, A generalized dynamic aerodynamic coefficient model for flight dynamics applications, 1997. (AIAA-97-3643)

[8] P.J. Gage, R.A. Stuckey, J.S. Drobik, A genetic approach to modelling flight dynamic characteristics, 35th Aerospace Sciences Meeting & Exhibit, 1997. (DOI: AIAA Paper 97-0536)

[9] M.G. Persovaa, Y.G. Soloveichik, V.K. Belov, et al, Modeling of aerodynamic heat flux and thermoelastic behavior of nose caps of hypersonic vehicles, Acta Astronaut. 136 (2017) 312-331. (DOI: 10.1016/j.actaastro.2017.02.021)

[10]S. Isaev, P. Baranov, I. Popov, et al, Improvement of aerodynamic characteristics of a thick airfoil with a vortex cell in sub- and transonic flow, Acta Astronaut. 132 (2017) 204-220. (DOI: 10.1016/j.actaastro.2016.11.029)

[11]J.C. Monfort, W.M. Whitcomb, High-attitude low-speed static aerodynamic characteristics of an f-4d fighter airplane model with leading-edge slats, NASA, 1975. (NASA TM X-62355)

[12]G. Peterson, W. Bond, R. Germann, et al, Using neural networks for aerodynamic parameter modeling, Proceedings of the American Control Conference, 1995. (DOI: WP13-3:50)

[13]D.I. Greenwell, A review of unsteady aerodynamic modelling for flight dynamics of manoeuvrable aircraft, AIAA Atmospheric Flight Mechanics Conference and Exhibit, 2004. (DOI: AIAA 2004-5276)

[14]T. Watanabe, K. Matsushima, K. Nakahashi, Aerodynamic shape optimization of a near-sonic passenger plane using computational fluid dynamics, P. I. Mech. Eng. G-J. Aer. 222 (2008) 1025-1035. (DOI: 10.1243/09544100JAERO349)

[15]S.L. Brunton, C.W. Rowley, D.R. Williams, Reduced-order unsteady aerodynamic models at low reynolds numbers, J. Fluid Mech. 724 (2013) 203-233. (DOI: 10.1017/jfm.2013.163)

[16]S. Bagherzadeh, M. Sabzeparvar, M. Karrari, Nonlinear aerodynamic model identification using empirical mode decomposition, P. I. Mech. Eng. G-J. Aer. 229 (2015) 1588-1605. (DOI: 10.1177/0954410014556112)

[17]M.D. Ortigueira, J.A.T. Machado, What is a fractional derivative? J. Comput. Phys. 293 (2015) 4-13. (DOI: 10.1016/j.jcp.2014.07.019)

[18]A. Palfalvi, Efficient solution of a vibration equation involving fractional derivatives, Int. J. Nonlin. Mech. 45 (2010) 169-175. (DOI: 10.1016/j.ijnonlinmec.2009.10.006)

[19]T.P. Sales, F.D. Marques, D.A. Pereira, et al, Dynamic assessment of nonlinear typical section aeroviscoelastic systems using fractional derivative-based viscoelastic model, J. Sound Vib. 423 (2018) 230-245. (DOI: 10.1016/j.jsv.2018.02.008)

[20]N. Ullah, W. Shaoping, M.I. Khattak, et al, Fractional order adaptive fuzzy sliding mode controller for a position servo system subjected to aerodynamic loading and nonlinearities, Aerosp. Sci. Technol. 43 (2015) 381-387. (DOI: 10.1016/j.ast.2015.03.020)

[21]O.W. Abdulwahhab, N.H. Abbas, A new method to tune a fractional-order pid controller for a twin rotor aerodynamic system, Arab J Sci Eng 42 (2017) 5179-5189. (DOI: 10.1007/s13369-017-2629-5)

[22]D. Hao, D.X. Li, Determination of dynamic mechanical properties of carbon black filled rubbers at wide frequency range using havriliak-negami model, Eur. J. Mech. A-Solid. (2015) 303-310. (DOI: 10.1016/j.euromechsol.2015.06.002)

[23]D. Hao, D.X. Li, Y.H. Liao, A finite viscoelastic constitutive model for filled rubber-like materials, Int. J. Solids Struct. (2015) 232-245. (DOI: 10.1016/j.ijsolstr.2015.04.002)

[24]D. Hao, D.X. Li, Y.H. Liao, Hyperelasticity, dynamic mechanical property, and rheology of addition-type silicone rubber (vpdms cured by pmhs), J. Appl. Polym. Sci. (2015) (DOI: 10.1002/APP.42036)

[25]D. Hao, D.X. Li, Y.H. Liao, Parameter identification of modified fractional zener model for thermorheological materials, J. Non-Cryst. Solids (2015) 106-119. (DOI: 10.1016/j.jnoncrysol.2014.11.015)

[26]D. Hao, L. Zhang, J. Yu, et al, Hyperelasticity of rubbery materials with chains' volume, nonaffine deformation, and topological constraint, IOP Conf. Series: Materials Science and Engineering 265 (2017) 12001. (DOI: 10.1088/1757-899X/265/1/012001)

[27]D. Hao, L. Zhang, J. Yu, et al, Dynamic characteristics of multifunctional structure for spacecraft, P. I. Mech. Eng. G-J. Aer. (2017) 1-7. (DOI: 10.1177/0954410017740384)

[28]D. Li, W. Liu, D. Hao, Vibration antiresonance design for a spacecraft multifunctional structure, Shock Vib. 2017 (2017) 1-10. (DOI: 10.1155/2017/5905684)

[29]D. Hao, L. Zhang, J. Yu, et al, Mechanical properties of multifunctional structure with viscoelastic components based on fve model, Acta Astronaut. (2018) 255-262. (DOI: 10.1016/j.actaastro.2017.11.043)

[30]D. Hao, L. Zhang, J. Yu, et al, Modeling of unsteady aerodynamic characteristics at high angles of attack, P. I. Mech. Eng. G-J. Aer. (2018) 1-11. (DOI: 10.1177/0954410018776527)

[31]M. Goman, A. Khrabrov, State-space representation of aerodynamic characteristics of an aircraft at high angles of attack, 1992. (DOI: AIAA-92-4651-CP)

[32]M. Goman, A. Khrabov, State-space representation of aerodynamic characteristics of an aircraft at high angles of attack, Journal of Aircraf 31 (1994) 1109-1115. (DOI:

[33]M.G. Goman, D.I. Greenwell, A.N. Khrabrov, The characteristic time constant approach for mathematical modelling of high angle of attack aerodynamics, The 22nd International Congress of Aeronautical Sciences, 2000. (DOI: Aug. 27-Sept. 1)

[34]E.J. Jumper, S.J. Schreck, R.L. Dimmick, Lift-curve characteristics for an airfoil pitching at constant rate, J. Aircraft 24 (1987) 680-687. (DOI:

[35]J.M. Brandon, Dynamic stall effects and application to high performance aircraft, AGARD Report No. 776 (1991) 1-2. (DOI:

[36]C. Hu, C.E. Lan, J. Brandon, Unsteady aerodynamic models for maneuvering aircraft, 1993. (AIAA-93-3626-CP)